Synthesis of nanoparticle-assembled tin oxide/polymer microcapsules†

Jie Yu,[a] Vinit S. Murthy,[a] Rohit K. Rana‡[a] and Michael S. Wong*[ab]

Received (in Berkeley, CA, USA) 10th October 2005, Accepted 16th January 2006
First published as an Advance Article on the web 30th January 2006
DOI: 10.1039/b513901e

Tin oxide nanoparticles can be assembled into micron-sized hollow capsule structures through a simple mixing procedure based on charge-mediated polymer aggregate templating.

Nanoparticle (NP) assembly represents a popular route towards the synthesis of advanced materials.[1,2] NPs can be prepared out of most compositions and in uniform sizes and shapes, and can exhibit useful size-dependent optical, electronic, and catalytic properties.[3] By treating NPs as building blocks for "supra-nanoparticulate" structures, *e.g.*, superlattices, microspheres, and nanowires,[2] one may be able to exploit these nanoscale properties for applications. We recently reported the assembly of silica NPs into micron-sized capsules using cationic polymer like polyallylamine hydrochloride (PAH) and multivalent anion like ethylenediaminetetraacetate (EDTA).[4,5] This NP assembly route occurs at room temperature, in water, and at mild pH values, allowing for the encapsulation of sensitive compounds without damage.[6] These nanoparticle-assembled capsules (NACs) should find uses in medicine, foods, and cosmetics, among others, as an alternative to vesicles and other hollow shell materials.

The silica NPs are not optically, electronically, or catalytically active, and neither are the silica microcapsules. Here, we describe the synthesis of semiconductor microcapsules using tin oxide (SnO_2) NPs, PAH, and phosphate anions, and show that the microcapsules exhibit the size-dependent optical properties of the SnO_2 NP building blocks. SnO_2 is a metal oxide semiconductor used in sensors, solar cells, photocatalysis, and displays.[7] A SnO_2-based material in a spherical shell construct could provide interesting functions to these applications as an optically active encapsulation device.

The general formation mechanism of NACs is a two-step process, as previously described.[4] Briefly, a cationic polymer solution (PAH) and a multivalent salt solution (phosphate) are combined, leading to a suspension of polymer aggegates in this first step (Scheme 1). The anion acts to crosslink ionically multiple PAH chains to form the aggregates. In the second step, the polymer aggregate suspension is combined with a NP sol; the negatively charged NPs (SnO_2 NPs) form a multi-layer-thick shell that is held together by the oppositely charged polymer. This formation route can be described as polymer aggregate templating.

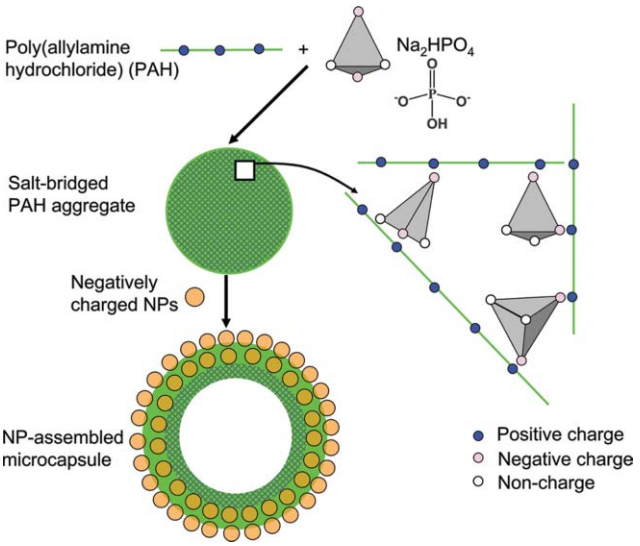

Scheme 1 Schematic of formation of SnO_2 microcapsules ("NACs") from SnO_2 NPs, PAH, and phosphate anions.

The interior of the NACs is filled by the polymer aggregate, but it can also be filled with just water, *i.e.*, no polymer in the core. The formation of the latter water-filled microcapsules is under investigation.

In the synthesis of SnO_2 NACs, 120 μl of a Na_2HPO_4 aqueous solution (0.01 M) is added to 20 μl of PAH water solution (2 mg/ml, molecular weight ~ 70 kDa) such that the charge ratio $R = 6$. R is defined as the ratio of total negative charge from phosphate to the total positive charge from PAH. The PAH–phosphate suspension (pH = 8.4) was mixed for 10 sec and left to age for 30 min. Then, 120 μl of SnO_2 NPs (1.6 wt% in water, Nyacol Nanotechnologies, Inc.) were added and mixed for 30 sec. The NPs measured 10–15 nm in hydrodynamic diameter (measured through dynamic light scattering, Brookhaven, ZetaPALS with BI-9000AT digital autocorrelator) and 5–10 nm in diameter through transmission electron microscopy (JEM 2010 with FasTEM system operating at 200 kV; Electronic Supplementary Information, Fig. S1). The zeta potential of these NPs (suspended in 0.01 M NaCl solution, pH ~ 8.7) was measured to be −22 mV (Brookhaven, ZetaPALS model), indicating the particle surface was negatively charged. The SnO_2 NPs were negatively charged because the pH values of the polymer aggregate suspension (~ 8.1) and the final NACs suspension (~ 8.4) were higher than the pH of point-of-zero charge of SnO_2 (pzc ~ 4–6).[8] The as-formed microcapsules, or NACs, were centrifuged and washed of excess NPs using water.

The SnO_2 NACs were characterized through TEM and scanning electron microscopy (FEI XL-30 Environmental SEM)

[a]*Department of Chemical and Biomolecular Engineering, Rice University, 6100 Main St., Houston, TX 77005-1892, USA*
[b]*Department of Chemistry, Rice University, 6100 Main St., Houston, TX 77005-1892, USA. E-mail: mswong@rice.edu; Fax: 01 713-348-5478; Tel: 01 713-348-3511*

† Electronic supplementary information (ESI) available: TEM image of SnO_2 NPs. XRD patterns of SnO_2 NPs and resultant SnO_2 microcapsules. See DOI: 10.1039/b513901e

‡ *Present address*: Indian Institute of Chemical Technology, Tarnaka, Hyderabad, AP, India 500007.

(Fig. 1a–d). They ranged in diameter size, from 500 nm to 3 μm, retaining their spherical shape after drying at room temperature and during microscopy. The shell structure was apparent in dark-field TEM (Fig. 1c). The shell thicknesses were approximately the same for the different sized NACs, at about 100 nm. There appeared to be a distribution in shell thicknesses, but this was not quantified. SnO_2 NPs are crystalline, and at higher magnifications, they could be identified as individual particles within the shell (Fig. 1d). The SnO_2 NPs are cassiterite (or tetragonal) crystal phase, according to powder X-ray diffraction (XRD) data (Electronic Supplementary Information, Fig. S2), with grain sizes of 3–4 nm. The smaller grain size values relative to NP size suggest the NPs are not perfect crystals, *e.g.*, twinning. XRD analysis further indicates that the microcapsules retained the crystal structure and grain size of the constituent SnO_2 NPs.

The location of the polymer was visualized by covalently binding to PAH the fluorescent molecule fluorescein isothiocyanate (FITC, ~ 1 FITC per chain). Suspended in water, the resulting NACs were spherical and shell-like under optical microscopy (Fig. 2a, Carl Zeiss, Axioplan2 model). In the same imaged NACs, the polymer was clearly present in the shell wall under confocal mode (Fig. 2b, laser-scanning confocal microscopy, Carl Zeiss, LSM 510 Meta model).

There is comparatively less polymer in the interior, which contributes to the hollow nature of the NACs. Thus, we consider these SnO_2 NACs to be water-filled microcapsules with shell walls composed of SnO_2 NPs and PAH. The volatiles content of these microcapsules (which is PAH) is ~ 40 wt%, according to thermogravimetric analysis (TGA, TA Instruments, DT 2960 model). The phosphate content was found to be ~ 10 wt%, based on inductively coupled plasma optical emission spectrometry (Perkin Elmer, OPTIMA-4300 DV model).

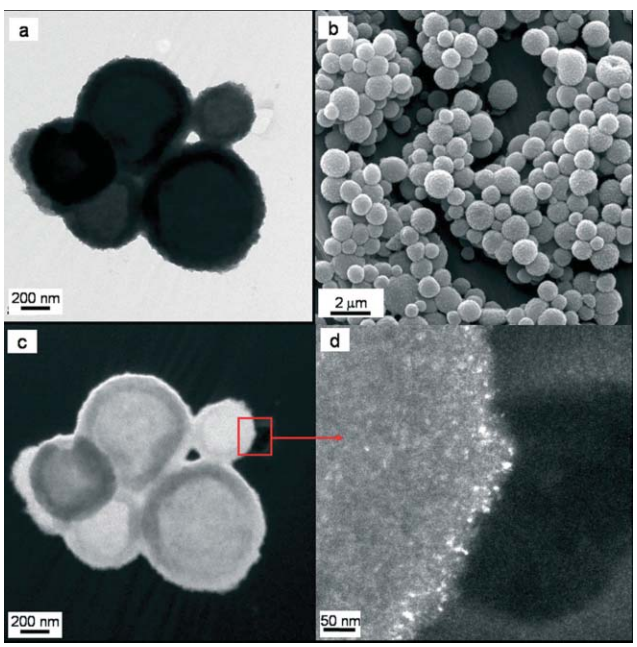

Fig. 1 (a) Brightfield TEM, (b) SEM, and (c,d) darkfield TEM images of SnO_2 NACs (prepared with PAH and phosphate anions, the white dots are contributed from SnO_2 NPs).

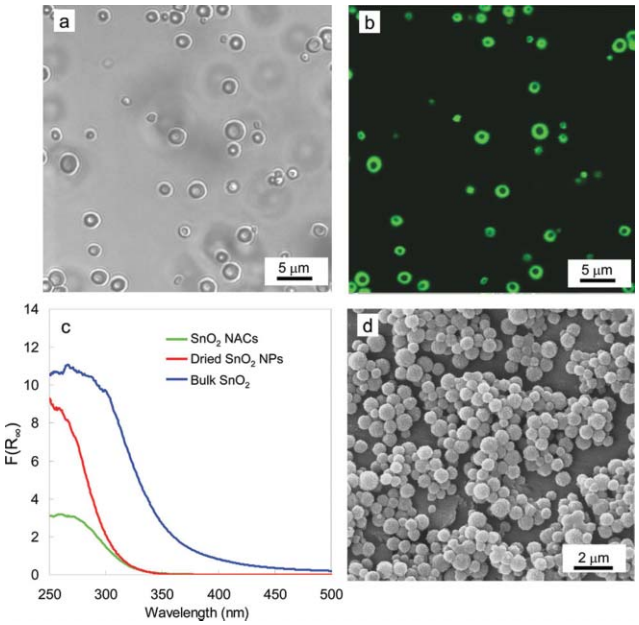

Fig. 2 (a) Brightfield optical and (b) confocal image of SnO_2 NACs (prepared with FITC-conjugated PAH and phosphate anions) suspended in water. (c) UV-vis spectra of SnO_2 NACs, dried SnO_2 NPs, and bulk SnO_2. (d) SEM of SnO_2 NACs prepared after aging PAH–phosphate aggregates for 5 min instead of 30 min.

The amount of SnO_2 NPs per microcapsule was estimated by assuming monodisperse microcapsules of 2 μm and an average NP size of 7 nm. The concentrations of typical as-synthesized NACs were measured in a range of 10^7–10^8 capsule/ml through Coulter counter measurements (Beckman Coulter, Multisizer III model). Based on these values and TGA analysis, mass balance calculations indicated that each microcapsule was comprised of 10^7–10^8 SnO_2 NPs.

The optical properties of SnO_2 NACs were measured using diffuse reflectance UV-vis spectroscopy (Shimadzu, UV2401-PC model; Harrick Praying Mantis diffuse reflectance attachment; MgO reference). From the diffuse reflectance UV-vis absorption spectra (in terms of Kubelka–Munk units $F(R_\infty)$[9]), SnO_2 NACs absorbed significantly only at wavelengths below 330 nm, similar to SnO_2 NPs (Fig. 2c). Bulk SnO_2, on the other hand, had a higher absorbance onset, at around 380 nm, indicative of a lower band gap energy E_0. Assuming the absorbance onset is due to a direct optical transition, then the band gap energies for bulk SnO_2, SnO_2 NPs, and SnO_2 NACs can be estimated (from $(F(R_\infty) \times hv)^2$ *vs.* hv curves) to be 3.7 eV, 4.1 eV, and 4.0 eV, respectively.[10] These values are consistent with the literature numbers of bulk SnO_2[11] and SnO_2 NPs.[12] Thus, SnO_2 NACs exhibit the optical properties of the SnO_2 NPs.

The average particle size of SnO_2 NACs could be adjusted using polymer aggregate aging time as the synthesis parameter (Table 1). The PAH–phosphate aggregates (R = 6) grow with aging time, which is consistent with other polymer–multivalent anion systems studied earlier, *e.g.*, poly(lysine)–citrate and PAH–ethylenediaminetetraacetate.[4] We recently showed that the polymer aggregates in general behave as charged colloidal species, consistent with the classical DLVO theory of colloid stability.[5] We also showed that these aggregates grow through a coalescence mechanism.[5]

This journal is © The Royal Society of Chemistry 2006

Table 1 Size characterization of polymer aggregates and microcapsules

Aging time (min)	Average hydrodynamic diameter of PAH–phosphate aggregates (nm)[a]	Average diameter of SnO_2 NACs (nm)[b]
2	517	580
5	595	620
10	678	720
15	724	800
20	755	880
25	822	1030
30	850	1110

[a] Based on size distribution measurements of aqueous suspensions. [b] 500 dried NAC particles counted for each sample *via* SEM.

The microcapsules—resulting from the addition of SnO_2 NPs to aggregate suspensions aged from 2 min to 30 min—increased in size with aggregate aging time (Table 1). The microcapsule sizes did not scale proportionally with polymer aggregate size, but this discrepancy could be easily attributed to increasing polydispersity of aggregates with aging time and the contraction of the NACs after drying (as observed for other NAC compositions[4]). While it is difficult to quantify all the effects of aggregate aging time on NAC structure (*e.g.*, shell thickness and SnO_2 NP per capsule), it is clear that microcapsule size can be controlled by aggregate aging time.

NAC synthesis is a versatile example of NP assembly, as guided by the templating action of cationic-polymer/anionic-salt aggregates. The structurally well-defined microcapsules are composed of SnO_2 NPs and polymer, are stable in suspension and in the dried form, and are simple to synthesize. These microcapsules exhibit the nanoscale optical properties of the semiconductor NP building blocks.

We acknowledge R. M. Yoo for helpful discussions and FITC–PAH conjugation, W. V. Knowles for TEM analysis, and M. O. Nutt for assistance with XRD analysis. We also gratefully acknowledge the financial support of Halliburton, Kraft Foods, and Rice University.

Notes and references

1 (*a*) Z. Tang and N. A. Kotov, *Adv. Mater.*, 2005, **17**, 951; (*b*) R. Shenhar, T. B. Norsten and V. M. Rotello, *Adv. Mater.*, 2005, **17**, 657; (*c*) S. A. Davis, M. Breulmann, K. H. Rhodes, B. Zhang and S. Mann, *Chem. Mater.*, 2001, **13**, 3218; (*d*) F. Caruso, *Chem.–Eur. J.*, 2000, **6**, 413; (*e*) P. T. Hammond, *Adv. Mater.*, 2004, **16**, 1271.

2 (*a*) H. Zeng, J. Li, J. Liu, Z. Wang and S. Sun, *Nature*, 2002, **420**, 395; (*b*) Y. Lalatonne, J. Richardi and M. P. Pileni, *Nat. Mater.*, 2004, **3**, 121; (*c*) W. A. Lopes and H. M. Jaeger, *Nature*, 2001, **414**, 735; (*d*) S. W. Lee, C. Mao, C. E. Flynn and A. M. Belcher, *Science*, 2002, **296**, 892; (*e*) A. Böker, Y. Lin, K. Chiapperini, R. Horowitz, M. Thompson, V. Carreon, T. Xu, C. Abetz, H. Skaff, A. D. Dinsmore, T. Emrick and T. P. Russell, *Nat. Mater.*, 2004, **3**, 302.

3 (*a*) A. Henglein, *Chem. Rev.*, 1989, **89**, 1861; (*b*) T. Trindade, P. O'Brien and N. L. Pickett, *Chem. Mater.*, 2001, **13**, 3843; (*c*) M. A. El-Sayed, *Acc. Chem. Res.*, 2001, **34**, 257; (*d*) K. Grieve, P. Mulvaney and F. Grieser, *Curr. Opin. Colloid Interface Sci.*, 2000, **5**, 168; (*e*) Al. L. Efros and M. Rosen, *Annu. Rev. Mater. Sci.*, 2000, **30**, 475.

4 R. K. Rana, V. S. Murthy, J. Yu and M. S. Wong, *Adv. Mater.*, 2005, **17**, 1145.

5 V. S. Murthy, R. K. Rana and M. S. Wong, *J. Phys. Chem. B*, submitted.

6 D. L. Wilcox, Sr., M. Berg, T. Bernat, D. Kellerman and J. K. Cochran, Jr., eds., *Hollow and Solid Spheres and Microspheres: Science and Technology Associated with Their Fabrication and Application*, Vol. 372, Mater. Res. Soc. Symp. Proc., Pittsburgh, PA: Materials Research Society, 1995.

7 (*a*) S. C. Glotzer, M. J. Soloman and N. A. Kotov, *AIChE J.*, 2004, **50**, 2978; (*b*) J. Dutta and H. Hofmann, in *Encyclopedia of Nanosci. Nanotech.*, Vol. 9, p. 617, H. S. Nalwa, ed., American Scientific Publishers, CA, 2004; (*c*) K. L. Chopra, S. Major and D. K. Pandya, *Thin Solid Films*, 1983, **102**, 1; (*d*) M. Grätzel, *Nature*, 2001, **414**, 338; (*e*) E. J. H. Lee, C. Ribeiro, T. R. Giraldi, E. Longo, E. R. Leite and J. A. Varela, *Appl. Phys. Lett.*, 2004, **84**, 1745; (*f*) H. M. Xiong, D. P. Liu, H. Zhang and J. S. Chen, *J. Mater. Chem.*, 2004, **14**, 2775; (*g*) J. Watson, *Sens. Actuators*, 1984, **5**, 29.

8 R. J. Hunter, *Foundations of Colloid Science*, 3rd edn., Oxford University Press, New York, 2001.

9 W. W. Wendlandt and H. G. Hecht, *Reflectance Spectroscopy*, Interscience Publisher, New York, 1966. The Kubelka–Munk unit is defined as $F(R_\infty) = (1 - R_\infty)^2/(2R_\infty)$, where R_∞ = (sample reflectance)/(MgO reflectance).

10 The band gap energy E_0, defined as the minimum photon energy required to excite an electron from the highest occupied molecular ortibal (HOMO) to the lowest unoccupied molecular orbital (LUMO), is the intercept of the fitted line through the $(F(R_\infty) \times h\nu)^2$ *vs.* $h\nu$ curve near the absorbance edge.

11 (*a*) R. Summitt, J. A. Marley and N. F. Borrelli, *J. Phys. Chem. Solids*, 1965, **25**, 1465; (*b*) T. Arai, *J. Phys. Soc. Jpn.*, 1960, **15**, 916; (*c*) K. B. Sundaram and G. K. Bhagavat, *J. Phys. D: Appl. Phys.*, 1981, **14**, 921; (*d*) K. C. Mishra, K. H. Johnson and P. C. Schmidt, *Phys. Rev. B: Condens. Matter*, 1995, **51**, 13927.

12 (*a*) P. Yang, D. Zhao, D. I. Margolese, B. F. Chmelka and G. D. Stucky, *Nature*, 1998, **396**, 152; (*b*) R. Dolbec, M. A. El Khakani, A. M. Serventi, M. Trudeau and R. G. Saint-Jacques, *Thin Solid Films*, 2002, **419**, 230; (*c*) V. P. Godbole, R. D. Vispute, S. M. Chaudhari, S. M. Kanetkar and S. B. Ogale, *J. Mater. Res.*, 1990, **5**, 372.